# Time-consistent non-rigid motion compensation for 3D DCE-MRI of the entire liver

Marijn van Stralen[1], Hanke J. Schalkx[2], Harriët W. Mulder[1], Kenneth Coenegrachts[3], Maarten S. van Leeuwen[2], Wouter B. Veldhuis[2], and Josien P.W. Pluim[1]
[1]*Image Sciences Institute, UMC Utrecht, Utrecht, Utrecht, Netherlands,* [2]*Radiology, UMC Utrecht, Utrecht, Utrecht, Netherlands,* [3]*Radiology, AZ St.‐Jan Brugge‐Oostende AV, Brugge, West-Vlaanderen, Belgium*

## Purpose

Recent developments have enabled high-resolution dynamic contrast-enhanced magnetic resonance imaging (DCE-MRI) of the entire liver. DCE-MRI is potentially a very sensitive tool for diagnosis and treatment of liver lesions, by mapping of their perfusion characteristics. However, breathing and other organ motion hampers the current clinical use of DCE-MRI for perfusion analysis. Moreover, intensity change as a result of contrast perfusion challenges existing motion correction techniques.
We propose a temporally consistent motion compensation method based on the integrated 3D + time alignment of the gradient magnitude of the image intensity.

## Methods

***Imaging*** Five consecutive patients without diffuse liver disease were evaluated with Gd-DTPA enhanced DCE-MRI for focal liver lesions. Patients were scanned on a Philips Achieva 1.5T MR scanner using a T1-weighted 4D-THRIVE [1] sequence (matrix=220x162, 100 slices, TR/TE=4.7/2.3ms, flip angle = 10°, FOV=395x296x200mm) during the first five minutes after contrast injection. Images of the entire liver were acquired with a temporal resolution of 2 seconds, in multiple breath-holds, resulting in a sequence of 16 frames in total within the first 5 minutes after contrast injection with a dense sampling in the early phases (see Fig. 1).

***Motion compensation*** DCE-MRI sequences were registered to compensate for patient motion, breathing motion and deformations caused by surrounding moving organs, such as the stomach. To this end, the sequences were first pairwise intensity-based registered using an affine transformation model to the unenhanced image in the sequence by optimizing normalized cross-correlation. Secondly, the affine registered sequences were non-rigidly registered using a 4D time-continuous registration with a B-spline deformation model and minimization of the gradient magnitude (GM) variance over time using an extension of [2]. A multi-resolution strategy with four levels and a final B-spline control point grid of 32mm was used. Random sampling with a stochastic optimizer kept computation manageable (~12 minutes per sequence). For comparison, the sequences were also registered with a temporally independently transformation and metric.

***Evaluation*** Manual segmentations of the liver were generated by slice-by-slice delineation of the outer contour on the unenhanced scan. In all the DCE-MRI frames the outer contour was manually drawn on three orthogonal slices through a manually chosen center-of-mass (CoM) of the liver. The quality of the registration was evaluated by measuring the point-to-surface distance of the transformed orthogonal contours to the full liver segmentation

## Results

Point-to-surface distances (P2S) were calculated for unregistered, 3D affine registered and 3D+time non-rigidly registered sequences. The mean results over the entire length of the DCE sequence, summarized over the patients are displayed in Table 1. It shows the improved alignment by the affine and B-spline registrations. The example qualitative results (Fig. 2) demonstrate the superiority of 3D + time B-spline registration over 3D affine registration.

## Discussion and conclusions

Previous work [3] has demonstrated the need for image registration to compensate for breathing motion in DCE-MRI exams of the liver. We present a novel time-consistent deformable registration method that improves alignment of relevant anatomy based on similarity of the gradient magnitude across the DCE-MRI sequence. The improved accuracy of the time-consistent method ('B-spline 3D+T') is shown in a direct comparison with its temporal independent counterpart ('B-spline 3D') and affine registration ('Affine 3D', see Table 1). The decreased performance of the independent 3D B-spline ('B-spline 3D') with respect to the 3D affine registration ('Affine 3D') illustrates the complexity of the registration task.
In contrast to [2], we do not assume temporal smoothness of the deformation field since the data is acquired in multiple (independent) breath-holds. However, the proposed method still supports this temporal continuity within a breath-hold, or in a free-breathing scenario. Also, the method is applicable to other perfusion imaging methods, such as dynamic susceptibility contrast (DSC) imaging and arterial spin labeling (ASL) and other organs (eg. kidney, pancreas, prostate).
The current evaluation focuses on validation of the transformation by measuring the spatial errors on the liver boundary. Although qualitative evidence also shows improved alignment of the organ's internals and compensation of other organ's motion (spleen, kidneys, etc.), this is not validated yet. Furthermore, the influence of motion compensation on pharmacokinetic modeling and the applicability of the current method on free-breathing acquisitions is ongoing work.

[1] Coenegrachts et al. Eur J Radiol 74(2010)529–535. [2] Metz et al. Med Image Analysis 15 (2011) 238-249. [3] Melbourne et al. Phys Med Biol 56 (2011) 7693-7708.

***Table 1.*** *Point-to-surface distances (N=5) for the different methods, measured for the three orthogonal liver contours to the reference 3D segmentation. All measurements are expressed as mean ± standard deviation in mm.*

| Method (N=5) | Mean | Median | StDev | Maximum |
|---|---|---|---|---|
| **Unregistered** | 3.0 ± 0.4 | 2.5 ± 0.3 | 2.4 ± 0.4 | 13.0 ± 2.8 |
| **Affine 3D** | 2.1 ± 0.1 | 1.6 ± 0.1 | 2.0 ± 0.3 | 11.7 ± 2.8 |
| **B-spline 3D** | 2.2 ± 0.3 | 1.6 ± 0.2 | 2.2 ± 0.6 | 12.7 ± 3.1 |
| **B-spline 3D+T** | **2.0 ± 0.1** | **1.5 ± 0.2** | **1.9 ± 0.2** | **11.8 ± 2.6** |

***Fig. 1.*** *Timing of the DCE-MRI sequence. 16 frames are acquired in seven breath-holds.*

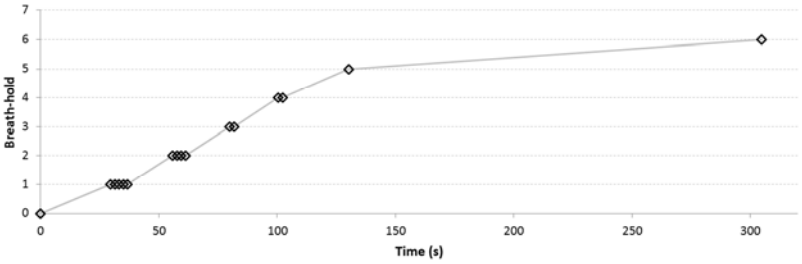


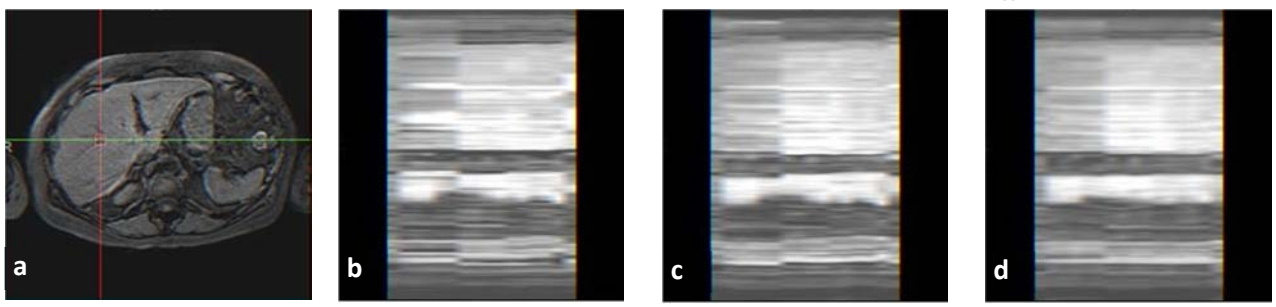


***Fig.2****. Visualization of the temporal consistence of the registration results.* ***a****. Axial slice with the line of interest in green.* ***b.*** *Temporal consistency of the unregistered data. The green line in a is on the vertical axis, the horizontal axis represents time.* ***c*** *and* ***d****. Temporal consistency of the affine and B-spline registrations, respectively.*